

# Unconfined compression properties of a porous poly(vinyl alcohol)-chitosan-based hydrogel after hydration

Si-Yuen Lee<sup>a,\*</sup>, Barry P. Pereira<sup>b</sup>, N. Yusof<sup>c</sup>, L. Selvaratnam<sup>d</sup>, Zou Yu<sup>b</sup>, A.A. Abbas<sup>a</sup>, T. Kamarul<sup>a</sup>

<sup>a</sup> Department of Orthopaedic Surgery, Faculty of Medicine, University of Malaya, 50603 Kuala Lumpur, Malaysia

<sup>b</sup> Musculoskeletal Research Laboratories, Department of Orthopaedic Surgery, Yong Loo Lin School of Medicine, National University of Singapore, Singapore 119074, Singapore

<sup>c</sup> Division of Agrotechnology and Biosciences, Malaysian Nuclear Agency, Ministry of Science, Technology and Innovation, Bangi, 43000 Kajang, Malaysia

<sup>d</sup> School of Medicine and Health Sciences, Monash University, Sunway Campus, 46150 Petaling Jaya, Malaysia

Received 21 July 2008; received in revised form 7 January 2009; accepted 10 February 2009

Available online 20 February 2009

## Abstract

A poly(vinyl alcohol) (PVA) hydrogel composite scaffold containing *N,O*-carboxymethylated chitosan (NOCC) was tested to assess its potential as a scaffold for cartilage tissue engineering in a weight-bearing environment. The mechanical properties under unconfined compression for different hydration periods were investigated. The effect of supplementing PVA with NOCC (20 wt.% PVA:5 vol.% NOCC) produced a porosity of 43.3% and this was compared against a non-porous PVA hydrogel (20 g PVA: 100 ml of water, control). Under non-hydrated conditions, the porous PVA–NOCC hydrogel behaved in a similar way to the control non-porous PVA hydrogel, with similar non-linear stress–strain response under unconfined compression (0–30% strain). After 7 days’ hydration, the porous hydrogel demonstrated a reduced stiffness (0.002 kPa, at 25% strain), resulting in a more linear stiffness relationship over a range of 0–30% strain. Poisson’s ratio for the hydrated non-porous and porous hydrogels ranged between 0.73 and 1.18, and 0.76 and 1.33, respectively, suggesting a greater fluid flow when loaded. The stress relaxation function for the porous hydrogel was affected by the hydration period (from 0 to 600 s); however the percentage stress relaxation regained by about 95%, after 1200 s for all hydration periods assessed. No significant differences were found between the different hydration periods between the porous hydrogels and control. The calculated aggregate modulus,  $H_A$ , for the porous hydrogel reduced drastically from 10.99 kPa in its non-hydrated state to about 0.001 kPa after 7 days’ hydration, with the calculated shear modulus reducing from 30.92 to 0.14 kPa, respectively. The porous PVA–NOCC hydrogel conformed to a biphasic, viscoelastic model, which has the desired properties required for any scaffold in cartilage tissue engineering.

© 2009 Acta Materialia Inc. Published by Elsevier Ltd. All rights reserved.

**Keywords:** Mechanical properties; Poly(vinyl alcohol)-chitosan-based hydrogel; Unconfined compression; Hydration effect; Cartilage regeneration

## 1. Introduction

Damaged articular cartilage has a limited ability to undergo self-repair and regenerate [1]. Recent studies have focused on the transplantation of a hybrid “scaffold cells” construct to encourage the cartilage regenerative process.

Several novel biomaterial scaffolds for the incorporation of cultured cells have since been proposed, including medical-grade polycaprolactone (mPCL) [2], bilayer type I/III collagen membrane [3], atelocollagen sponge/poly-L-lactic acid (PLLA) mesh composite [4], poly(D,L)-lactide-co-glycolide (PLGA)-based biomaterials [5] and fibrin glue [6,8]. Apart from ensuring that cultured cells incorporate into suitable biodegradable scaffolds, another important issue is to ensure that the scaffold mimics the structural properties of the native tissue and are able to withstand

\* Corresponding author. Tel.: +60 19 353 3830; fax: +60 37 967 7536.

E-mail address: [siyuen\\_lee@yahoo.com](mailto:siyuen_lee@yahoo.com) (S.-Y. Lee).

the loading environment of the recipient site. Recently, the use of hydrogels as a scaffold for articular cartilage regeneration has offered an attractive and promising approach. Their ability to maintain a high water content, biocompatibility, permeability, hydrophilicity, tissue-like elasticity and low coefficient of friction are among of the advantages of hydrogels. This enables the hydrogels to resemble the structural properties of cartilage extracellular matrix [7–15].

The choice of using an implanted material to replace a biological tissue-like the articular cartilage depends on the material's ability to behave in a way that is similar to the tissue it is replacing. Although, hydrogels have been used in a wide range of biomedical applications including contact lenses [7], corneal implants [8], drug delivery [9,10], adhesives [11], artificial menisci [12] and substitutes for skin, ligament, tendon, cartilage and bone [13–15]; their major drawback is the limited use under weight-bearing conditions. Current work has progressed to develop hydrogel composite scaffolds to be used as a construct for seeding cells. This is done by blending two or more polymers with the aim of obtaining a viscoelastic and interconnecting porous structure that will provide a more compliable biphasic material when hydrated. The key criterion is that the replacement biomaterial is expected to maintain the structural integrity of the tissue it is to replace, and this is during the course of the repair and regeneration phases. The mechanical properties of hydrogels are generally poor; although these biomaterials possess many attractive features for biomedical applications [16].

Poly(vinyl alcohol) (PVA), one of the most widely used polymers, is known for its excellent weight-bearing properties and biocompatibility [8,12,17–19]. Stammen et al. [14] found that PVA hydrogels formed via freeze–thawing possessed compressive and tensile mechanical properties comparable to native articular cartilage in the knee. PVA can be prepared as a porous structure. Highly porous PVA hydrogels are prepared in a variety of ways including the addition of porosogens such as sucrose, sodium chloride and polyethylene glycolic acid (PEG) [20]. Our group has synthesized porous PVA hydrogel by blending a low molecular weight of PVA with *N,O*-carboxymethylated chitosan (NOCC), and without the use of porosogens. Chitosan has a similar structure to glycosaminoglycans (GAGs), a key component of cartilage extracellular matrix. The incorporation of natural polymer such as chitosan and gelatin can also improve the degradation of a biomaterial [19]. We hypothesized that PVA–NOCC scaffold with appropriate interconnecting pores will ensure a biphasic property when hydrated, thus qualifying this scaffold as a potential candidate for cartilage tissue engineering [21–23].

This study investigates the behavior of a highly porous, NOCC supplemented PVA hydrogel (PVA–NOCC) under compression and determines their viscoelastic properties and Poisson's ratio when hydrated under unconfined compression [24–32]. The PVA hydrogel without any additives under the same loading and hydration conditions will be

used as a control for comparison. The main aim of this study is to assess the feasibility of this porous PVA–NOCC hydrogel as a potential extracellular matrix scaffold for future cell implantation in cartilage tissue engineering to repair the damaged cartilage in load-bearing joints.

## 2. Materials and methods

### 2.1. Preparation of hydrogels

PVA-117 ( $M_w = 74,000 \text{ g mol}^{-1}$ ) was obtained from Kuraray Co. Ltd, Japan. NOCC was obtained from the Standards and Industrial Research Institute (SIRIM), Malaysia. The porous hydrogel was prepared by blending PVA with NOCC in the ratio (w/v) of 20% PVA to 5% NOCC. The control PVA hydrogel was prepared as 20% PVA in distilled water. The polymer solutions were then cast into cylindrical molds and physically cross-linked by irradiation at 50 kGy. The hydrogels were frozen at  $-80^\circ\text{C}$  for 24 h prior to lyophilization. Subsequently, the hydrogels were cut into disks approximately 2 mm in height, with a diameter of 5 mm. The porosity of the specimens was sampled and assessed using an electron microscope (FEI Quanta 400, USA) and was found to be on average 43.3% (SD, 13.9%). The average pore sizes ranged from small (with a mean relative diameter of 18.13  $\mu\text{m}$ ; SD, 3.28  $\mu\text{m}$ ), medium (35.27  $\mu\text{m}$ ; SD, 3.06  $\mu\text{m}$ ) and large (78.91  $\mu\text{m}$ ; SD, 5.41  $\mu\text{m}$ ). The control PVA had no pores.

### 2.2. Unconfined compression test

The hydrogel composite samples ( $n = 18$ ) were immersed in Dulbecco's Modified Eagle's Medium (DMEM) (pH 7.4) at  $37^\circ\text{C}$ . Unconfined compression tests were performed at 1, 3 and 7 days after immersion [24]. Samples at day 0 were also included, and this involved only the hydrogel composite without it being immersed in DMEM. The initial diameter and thickness of hydrogel composites at day 0 were measured using a vernier caliper and a micrometer, respectively. Samples were then loaded in between two impermeable, unlubricated compression platens using a universal testing machine (Instron Model 5543, MA, USA) with the top platen coupled to a 50 N capacity load cell and a machine actuator. Samples were compressed at a strain rate of 100% strain  $\text{min}^{-1}$  until a 30% compressive strain, before being unloaded. Both the tangent compressive modulus and compressive stress values were calculated at 15%, 20% and 25% compressive strain for each sample over the periods of hydration (1, 3 and 7 days). Poisson's ratio,  $\nu$ , was obtained by directly measuring the lateral expansion in unconfined compression test at 30% compressive strain using an optical method as previously described by Jurvelin et al. [28–31]. Briefly, this involved taking a digital image at the end point of compression, against a calibrated grid. The grid was used to estimate the change in the height and width of the specimen. Potential optical distortions were minimized by using

the central region of the image field, with the calibrated grid placed in the same plane as the sample. A commercial grade silicone was used to validate the system and demonstrate a Poisson's ratio of 0.5 (see Section 2.4 for a description of image analysis) [26].

The aggregate modulus ( $H_A$ ) was indirectly estimated by applying the following equation:

$$H_A = \frac{1-v}{(1+v)(1-2v)} E_s$$

where  $E_s$  is the tangent compressive modulus, obtained at the 25% compressive strain from the regression analysis fit to the data points [24].

### 2.3. Stress relaxation test

Hydrogel composite samples were immersed in DMEM in a Petri dish and load applied using an indentation technique (impervious, plane-ended, smooth stainless steel, cylindrical indenter, diameter 1.0 mm) at a rate of 100% strain  $\text{min}^{-1}$  and held at 30% compressive strain for 1200 s, with the applied load (N) recorded to determine the stress relaxation response. The applied load as a percentage of the peak load (i.e. the stress relaxation response) was plotted over the period of compressive strain for each period of hydration (days) [26]. The shear modulus,  $\mu$ , was calculated at 30% compressive strain in the fixed displacement mode, from the following relationship [25]:

$$\mu = \frac{P(1-v)}{4a\omega\kappa}$$

based on the applied peak load,  $P$ , indentation geometry (aspect ratio,  $a/h$ ), the Poisson's ratio,  $v$ , estimated from the optical measurement and the correction factor,  $\kappa$ , obtained from Hayes et al. [33] where  $h$  = thickness of specimen,  $a$  = indentation radius (0.8 mm),  $\omega$  = indentation depth (30% compressive strain).

### 2.4. Data and statistical analysis

All data are presented as the mean and standard errors of means based on the sample size of each group (PVA, PVA–NOCC) against the treatments (hydration periods: 0 days, 1, 3 and 7 days) tested. The non-linear stress–strain data from the unconfined compression test up to a 30% compression strain were curve-fitted according to the following non-linear equation [26]:

$$\sigma = A(e^{B\varepsilon}-1)$$

Regression modulus and compressive stress were calculated at 15%, 20% and 25% compressive strain from this non-linear relationship. The toe-region modulus was also calculated. Stress relaxation curves were plotted as percent relaxation ( $\sigma_E/\sigma_p \times 100$ ), where  $\sigma_E$  is the equilibrated stress measured at 30% compressive strain over time, and  $\sigma_p$  is the peak equilibrium stress recorded over the time of loading.

Imaging tools (Adobe Photoshop 7.0, Adobe Systems Inc., San Jose, CA) were utilized to estimate sample diameter, and width at the time points for calculating Poisson's ratio. The photo resolution was measured as 0.008 mm pixel $^{-1}$ . As the disk-shaped specimen bulged at mid-height, the diameter of each image was measured at five locations along the length, and the lateral strain ( $\varepsilon_l$ ) calculated as the change in the mean diameter at 30% compression strain over the initial diameter of the cylindrical sample [25–28]. As the specimens were cylindrical in shape, the measurement of the maximum diameter (width) corresponding to the central plane, which had a barreling effect, was a limitation in our estimation. Axial strain ( $\varepsilon$ ) was calculated at 30% compression strain, based on the cross-head displacement over the initial height. The Poisson's ratio was estimated as the ratio between lateral strain and axial strain ( $\varepsilon_l/\varepsilon$ ).

Analysis of variance (ANOVA) was used to compare PVA and PVA–NOCC, and against the different treatments (1, 3 and 7 day hydration periods) with a post hoc Scheffé test used to compare each set of data. All statistical analyses were carried out using statistical software (SPSS 15.0 for Windows, SPSS Inc., Chicago, IL).

## 3. Results and discussion

### 3.1. Unconfined compression test

Under unconfined compression, both the non-hydrated and hydrated PVA hydrogels typically showed a non-linear stress–strain response (Fig. 1A). The non-hydrated PVA–NOCC hydrogels showed the expected non-linear behavior as well, but with hydration the slope of the stress–strain curve was reduced by an order of 100, displaying a more linear stress–strain relationship (Fig. 1B).

The mean compressive stress and stiffness obtained from the regression analysis fit of the stress–strain curves at 15%, 20% and 25% compressive strain, including the toe-region stiffness, are summarized in Table 1. At each compressive strain, the compressive stiffness was significantly different for the various periods of hydration for PVA (ANOVA,  $P < 0.001$ ) and PVA–NOCC (ANOVA,  $P < 0.001$ ). The stiffness and compressive stress of PVA and PVA–NOCC did not differ in their non-hydrated state. When hydrated for 1, 3 and 7 days, PVA–NOCC had a significantly lower stiffness (ANOVA,  $P < 0.001$ ) and compressive stress (ANOVA,  $P < 0.001$ ) compared to PVA at 15%, 20% and 25% compressive strain respectively.

Both the non-hydrated porous PVA–NOCC and the non-porous control PVA hydrogels were noted to possess a non-linear behavior at the initiation of strain, suggesting an isotropic elastic model (Fig. 1). The different slope of the curve (i.e. the Young's modulus) is attributed to the different polymer content. The control PVA hydrogel, in a solid gel form, did not have any pores, while the PVA–NOCC hydrogel, fabricated with a porosity of 43.3%, had inter-

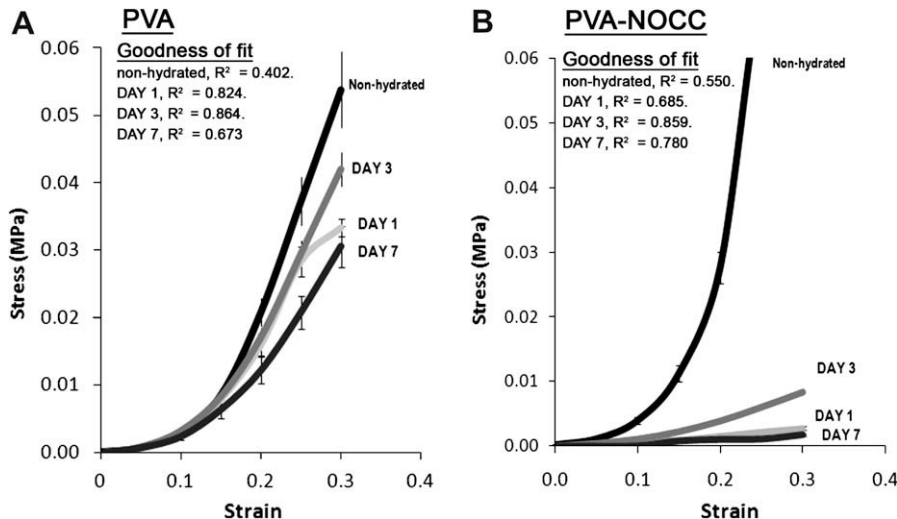


Fig. 1. Stress-strain curve of the two hydrogels under unconfined compression: (A) PVA, (B) PVA-NOCC hydrated in Dulbecco's Modified Eagle's Medium (DMEM) for different periods (pH 7.4), at 37 °C. The data were fitted with a non-linear equation,  $\sigma = A(e^{Bx-1})$ , with  $R$ -square used as the goodness of fit. (An  $R$ -square value of 0.864 means that the fit of the curve explains 86.4% of the total variation in the data about the mean. A value of closer to 1 indicates a better curve fit.)

Table 1

Summary of mean compressive stiffness ( $K$ ) and compressive stress ( $\sigma$ ) at various strain levels (%) obtained from the regression analysis of the stress–strain curves for the two hydrogels (PVA, PVA–NOCC), over 1, 3 and 7 days of hydration, compared to the non-hydrated specimen at day 0. All values in kPa reported as mean (standard error of mean).

	Compressive stiffness (kPa) and compressive stress (kPa)					
	Non-hydrated	Day 1	Day 3	Day 7	ANOVA	
PVA	$K_{\text{toe region}}$	0.567 (0.01)	0.112 (0.01)	0.109 (0.01)	0.092 (0.01)	$P < 0.001$
	$K_{15\%}$	1.082 (0.02)	0.292 (0.01)	0.309 (0.01)	0.226 (0.01)	$P < 0.001$
	$K_{20\%}$	1.495 (0.03)	0.473 (0.01)	0.518 (0.01)	0.355 (0.01)	$P < 0.001$
	$K_{25\%}$	2.066 (0.04)	0.766 (0.01)	0.870 (0.01)	0.557 (0.02)	$P < 0.001$
	$\sigma_{15\%}$	8.51 (0.94)	7.95 (0.94)	8.39 (0.72)	6.41 (1.33)	$P < 0.001$
	$\sigma_{20\%}$	20.82 (2.06)	16.00 (1.62)	17.17 (1.30)	12.24 (1.99)	$P < 0.001$
	$\sigma_{25\%}$	37.28 (3.61)	28.36 (2.22)	29.56 (1.95)	20.83 (2.44)	$P < 0.001$
PVA-NOCC	$K_{\text{toe region}}$	0.372 (0.01)	0.002 (0.01)	0.008 (0.01)	0.000 (0.01)	$P < 0.001$
	$K_{15\%}$	1.139 (0.02)	0.004 (0.01)	0.020 (0.01)	0.001 (0.01)	$P < 0.001$
	$K_{20\%}$	1.992 (0.04)	0.005 (0.01)	0.031 (0.01)	0.001 (0.01)	$P < 0.001$
	$K_{25\%}$	3.484 (0.07)	0.008 (0.01)	0.049 (0.01)	0.002 (0.01)	$P < 0.001$
	$\sigma_{15\%}$	11.21 (1.2)	0.94 (0.13)	2.22 (0.21)	0.78 (0.10)	$P < 0.001$
	$\sigma_{20\%}$	27.62 (2.44)	1.56 (0.17)	3.89 (0.29)	1.00 (0.00)	$P < 0.001$
	$\sigma_{25\%}$	72.16 (5.13)	2.19 (0.19)	6.06 (0.37)	1.06 (0.06)	$P < 0.001$

connecting pores of varying sizes. Changes in polymer content and its porosity would change both physical and material properties of the hydrogels, and this was seen with the significantly low compressive stiffness and compressive stress measured for porous PVA–NOCC hydrogel. With hydration, the compressive stress and stiffness increased from day 1 to day 3 of hydration and then decreased after day 7 for both the PVA control and porous PVA–NOCC hydrogels, attributed to the equilibrium of the hydrogel material system with water [27].

### 3.2. Poisson's ratio

The thickness, Poisson's ratio, aggregate modulus,  $H_A$ , (kPa) and the shear modulus ( $\mu$ ) obtained indirectly from

the unconfined compression test are summarized in Table 2. At 30% unconfined axial compression, the PVA hydrogels were found to maintain a mean Poisson's ratio of 0.86, irrespective of the period of hydration (ANOVA,  $F = 2.035$ ,  $P = 0.41$ , Scheffé's post hoc test). PVA–NOCC hydrogels showed a different trend (Fig. 2), their Poisson's ratio increased by more than two-fold from the non-hydrated state to hydrated state after 1 day of hydration ( $P < 0.001$ ). After 3 days of hydration, the changes were not significant ( $F = 0.49$ ,  $P = 0.34$ ), the Poisson's ratio being approximately 0.8. With 7 days of hydration, the Poisson's ratio for PVA–NOCC hydrogels further increased to 1.33 ( $F = 8.83$ ,  $P < 0.001$ ), suggesting that a change in the volume of the specimen during loading (given that the value was greater than 1).

Table 2

Summary of thickness (mm), Poisson's ratio, aggregate modulus (kPa) and shear modulus (kPa) estimated at 30% compression strain from the unconfined compression test.

	Non-hydrated	Period of hydration		
		Day 1	Day 3	Day 7
<b>PVA</b>				
Thickness, $t$ (mm)	1.37 (0.10)	1.57 (0.06)	2.00 (0.00)	1.53 (0.03)
Poisson's ratio, $\nu$	0.70 (0.10)	0.84 (0.16)	1.18 (0.24)	0.73 (0.15)
Aggregate modulus, $H_A$ (kPa)	1.76 (0.06)	0.26 (0.02)	0.15 (0.02)	0.48 (0.03)
Shear modulus, $\mu$ (kPa)	5.17 ( $1.7 \times 10^{-6}$ )	1.48 ( $2.1 \times 10^{-7}$ )	1.40 ( $2.0 \times 10^{-7}$ )	2.39 ( $6.2 \times 10^{-7}$ )
<b>PVA-NOCC</b>				
Thickness (mm)	1.19 (0.03)	1.44 (0.07)	1.00 (0.00)	1.48 (0.04)
Poisson ratio, $\nu$	0.12 (0.06)	0.76 (0.10)	0.77 (0.35)	1.33 (0.12)
Aggregate modulus, $H_A$ (kPa)	10.99 (0.07)	0.01 (0.001)	0.03 (0.001)	0.001 (0.00)
Shear modulus, $\mu$ (kPa)	30.92 ( $1.9 \times 10^{-5}$ )	0.20 ( $5.5 \times 10^{-9}$ )	0.85 ( $2.6 \times 10^{-8}$ )	0.14 ( $1.3 \times 10^{-6}$ )

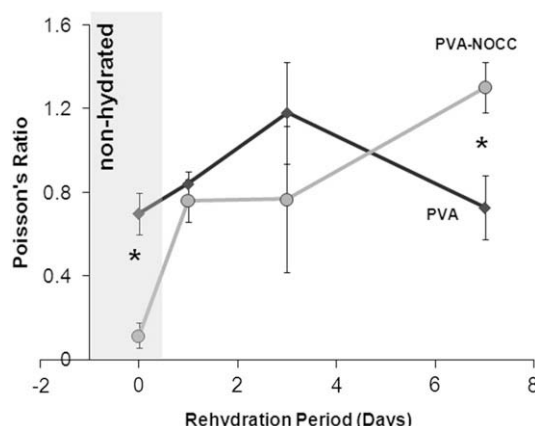


Fig. 2. Change in Poisson ratio of the hydrogels over the period of hydration in Dulbecco's Modified Eagles Medium (DMEM) (pH 7.4) at 37 °C. Statistically significant values between the two hydrogels at various time points are indicated with an asterisk (ANOVA,  $P < 0.001$ ).

After 7 days, PVA-NOCC hydrogels had a Poisson's ratio that was 1.7 times more than that of PVA hydrogels. The mean aggregate modulus and mean shear modulus had increased for PVA between day 1 ( $H_A = 0.26$  kPa,  $\mu = 1.48$  kPa) and day 7 ( $H_A = 0.48$  kPa,  $\mu = 2.39$  kPa) of hydration, while for PVA-NOCC hydrogels, the aggregate stiffness and shear modulus were noted to decrease between day 1 ( $H_A = 0.01$  kPa,  $\mu = 0.2$  kPa) and day 7 ( $H_A = 0.001$  kPa,  $\mu = 0.14$  kPa) of hydration.

The PVA material demonstrated higher Poisson's ratios with longer periods of hydration for both the non-porous PVA (0.73–1.18) and the porous PVA-NOCC: (0.76–1.33). These higher values are associated with an increase in volume due to swelling of the hydrogel constantly bathed in DMEM. This range differs from the other reports where the Poisson's ratio would be between 0.33 and 0.5 [31,32], the latter values complying constant volume. However, it should be noted that the PVA used had a molecular weight of 74,000 g mol<sup>-1</sup> and a blend of 20% PVA in distilled water, and so it would be necessary to always compare the type of PVA hydrogel used. It is clear that the specific constituent the PVA use will determine the level

of swelling. It is interesting to note that Urayama et al. [32] also demonstrated that the Poisson's ratio for PVA would vary with the solvent flow during hydration and when compressed, as well as its porosity.

What was of interest was that the Poisson's ratio demonstrated for the hydrated PVA material used in this study falls within the range of that reported for normal articular cartilage (0.62–1.87) [24,28–30].

### 3.3. Stress relaxation test

The stress relaxation function differed between PVA (Fig. 3A) and PVA-NOCC (Fig. 3B) hydrogels. No significant differences were found between the different periods of hydration for both hydrogels, but it was observed that toward 1200 s, the percentage relaxation regained about 95% for all periods of hydration. For PVA-NOCC hydrogels, between 100 s and 800 s, a drop in the relaxation percentage for day 1 and day 7 of hydration to about 75% (~600 s) was observed, and then returning to the equilibrium state of 100% with time. Although PVA-NOCC took a longer time to regain equilibrium, the hydrogel showed distinct viscoelastic properties. Its viscoelastic behavior makes it suitable for cartilage cells or chondrocyte seeding.

The data presented here confirmed that the mechanical properties of porous PVA-NOCC hydrogels depend primarily on polymer content and concentration. Their weight–volume ratios are expected to affect the compressive modulus, stiffness and relaxation values [34]. Better mechanical properties of PVA-NOCC hydrogel could be achieved by increasing the ratio of PVA.

## 4. Conclusion

In conclusion, the mechanical behavior of the two hydrogels under unconfined compression demonstrated that PVA-NOCC holds much potential as a scaffold for implantation of cultured cells with the aim of regenerating cartilage in a weight-bearing joint defect. It may achieve better cartilage mechanical function following glycosaminoglycans production in chondrocyte culture as the data shown here

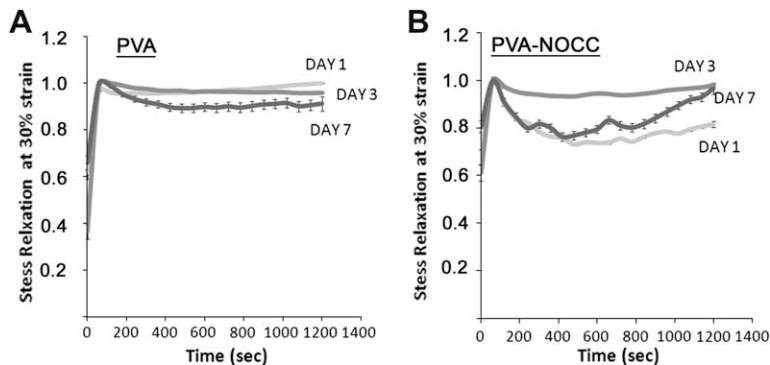


Fig. 3. Stress relaxation curves of (A) PVA and (B) PVA-NOCC hydrogels immersed in DMEM in a Petri dish and loaded using the indentation technique (impermeable, plane-ended, smooth stainless steel, cylindrical indenter, diameter 1.0 mm) at a rate of 100% strain min<sup>-1</sup> and held at 30% compressive strain for 1200 s. 1.0 on the y axis corresponds to the appropriate compressive stress value at 30% strain for each of the rest days.

are for unseeded hydrogels. Future work should include investigation of PVA-NOCC with different concentration groups, unconfined compression and confined compression testing on chondrocyte seeded hydrogels and cellular interaction. This study provided valuable information on the structural peculiarities of PVA-chitosan-based hydrogels. The evaluation of the hydration effect can be considered as a crucial step towards the optimal design of this material for cartilage tissue engineering applications.

## Acknowledgements

This project was funded by the University of Malaya Fundamental Grant (FP 050/2005D) and Science Fund (13-02-03-3042) from the Ministry of Science, Technology and Innovation Malaysia (MOSTI). The authors would like to thank the Head, Department of Orthopaedic Surgery, National University of Singapore for supporting this collaborative work, conducted at the Musculoskeletal Research Laboratories, NUS, as well as Asnah Hassan from Malaysian Nuclear Agency for technical support.

## References

- [1] Buckwalter JA, Mankin HJ. Articular cartilage repair and transplantation. *Arthritis Rheum* 1998;41:1331–42.
- [2] Shao XX, Hutmacher DW, Ho ST, Goh JCH, Lee EH. Evaluation of a hybrid scaffold/cell construct repair of high load bearing osteochondral defects in rabbits. *Biomaterials* 2006;27:1071–80.
- [3] Willers C, Chen J, Wood D, Xu J, Zheng MH. Autologous chondrocytes implantation with collagen bioscaffold for the treatment of osteochondral defects in rabbits. *Tiss Eng* 2005;11:1065–76.
- [4] Ito Y, Ochi M, Adachi N, Sugawara K, Yanada S, Ikada Y, et al. Repair of osteochondral defect with tissue engineered chondral plug in rabbit model. *Arthroscopy* 2005;21:1155–63.
- [5] Niederauer GG, Slivka MA, Leatherbury NC, Korvick DL, Harroff Jr HH, Ehler WC, et al. Evaluation of multiphase implants for repair of focal osteochondral defects in goats. *Biomaterials* 2000;21:2561–74.
- [6] Van Susante JLC, Buma P, Schuman L, Homminga GN, Van Den Berg WB, Veth RPH. Resurfacing potential of heterologous chondrocytes suspended in fibrin glue in large full-thickness defects of femoral articular cartilage: an experimental study in the goat. *Biomaterials* 1999;20:1167–75.
- [7] Berry M, Harris A, Corfield AP. Patterns of mucin adherence to contact lenses. *Invest Ophthalmol Vis Sci* 2003;44:567–72.
- [8] Vijayasekaran S, Fitton JH, Hicks CR, Chirila TV, Crawford GJ, Constable IJ. Cell viability and inflammatory response in hydrogel sponges implanted in the rabbit cornea. *Biomaterials* 1998;19:2255–67.
- [9] Li J, Ni XP, Leong KW. Injectable drug-delivery systems based on supramolecular hydrogels formed by poly(ethylene oxide) and alpha-cyclodextrin. *J Biomed Mater Res* 2003;65A:196–202.
- [10] Rodriguez R, Alvarez-Lozano C, Concheiro A. Cationic cellulose hydrogels: kinetics of the cross-linking process and characterization as pH/ion-sensitive drug delivery systems. *J Control Release* 2003;86:253–65.
- [11] Skelhorne G, Munro H. Hydrogel adhesives for wound-care applications. *Med Device Technol* 2002;3:19–23.
- [12] Kobayashi M, Toguchida J, Oka M. Preliminary study of polyvinyl-alcohol-hydrogel (PVAH) artificial meniscus. *Biomaterials* 2003;24:639–47.
- [13] Young CD, Wu JR, Tsou TL. High-strength, ultra-thin and fiber-reinforced pHEMA artificial skin. *Biomaterials* 1998;19:1745–52.
- [14] Stammen JA, Williams S, Ku DN, Gulberg RE. Mechanical properties of a novel PVA hydrogel in shear an unconfined compression. *Biomaterials* 2001;23:799–806.
- [15] Bryant SJ, Anseth KS. Controlling the spatial distribution of ECM components in degradable PEG hydrogels for tissue engineering cartilage. *J Biomed Mater Res* 2003;64A:70–9.
- [16] Corkhill PH, Trevett AS, Tighe BJ. The potential of hydrogels as synthetic articular cartilage. *Proc Inst Mech Engrs* 1990;204:147–55.
- [17] Tamura K, Ike O, Hitomi S, Isobe J, Shimizu Y, Nambu M. A new hydrogel and its medical application. *Trans Amer Soc Artif Organs* 1986;32:605–8.
- [18] Fujimoto K, Minato M, Ikada Y. In: Shalaby SW, Ikada Y, Langer R, Williams J, editors. Polymers of biological and biomedical significance. ACS symposium series 540. New York: Plenum Press; 1994. p. 228–41.
- [19] Wang M, Li Y, Wu J, Xu F, Zuo Y, Jansen JA. In vitro and in vivo study to the biocompatibility and biodegradation of hydroxyapatite/poly(vinyl alcohol)/gelatin composite. *J Biomed Mater Res A* 2008;85:418–26.
- [20] Peppas NA, Simmons REP. Mechanistic analysis of protein delivery from porous polyvinyl alcohol system. *J Drug Del Sci Tech* 2004;14:285–9.
- [21] Griffon DJ, Reza-Sedighi M, Schaeffer DV, Eurell JA, Johnson AL. Chitosan scaffold: interconnective pore size and cartilage engineering. *Acta Biomaterialia* 2006;2:313–20.
- [22] Hoemann C, Sun J, Legare A, McKee M, Bushmann M. Tissue engineering of cartilage using an injectable and adhesive chitosan-based cell-delivery vehicle. *Osteoarthritis Cartilage* 2005;13:318–29.

- [23] Elder SH, Nettles DL, Bumgardner JD. Synthesis and characterization of chitosan scaffolds for cartilage fibers for potential use in cartilage-tissue engineering. *Meth Mol Biol* 2004;238:41–8.
- [24] Korhonen RK, Laasanen MS, Toyras J, Rieppo J, Hirvonen J, Helminen HJ, et al. Comparison of the equilibrium response of articular cartilage in unconfined compression, confined compression and indentation. *J Biomech* 2002;35:903–9.
- [25] Jurvelin JS, Arokoski JPA, Hunziker EB, Helminen HJ. Topographical variation of the elastic properties of articular cartilage in canine knee. *J Biomech* 2000;33:669–75.
- [26] Cloyd JM, Malhotra NR, Weng L, Chen W, Mauck RL, Elliott DM. Material properties in unconfined compression of human nucleus pulposus, injectable hyaluronic acid-based hydrogels and tissue engineering scaffolds. *Eur Spine J* 2007;16:1892–8.
- [27] Thomas J, Lowman A, Marcolongo MJ. Novel associated hydrogels for nucleus pulposus replacement. *Biomater Res* 2003;67A:1329–37.
- [28] Jurvelin JS, Buschmann MD, Hunziker EB. Optical and mechanical determination of Poisson's ratio of adult bovine humeral articular cartilage. *J Biomech* 1997;30:235–41.
- [29] Wang CC, Chahine NO, Hung CT, Ateshian GA. Optical determination of anisotropic material properties of bovine articular cartilage in compression. *J Biomech* 2003;36:339–53.
- [30] Kelly TA, Ng KW, Wang CC, Ateshian GA, Hung CT. Spatial and temporal development of chondrocyte-seeded agarose constructs in free-swelling and dynamically loaded cultures. *J Biomech* 2006;39:1489–97.
- [31] Elliott DM, Narmoneva DA, Setton LA. Direct measurement of the Poisson's ratio of human patella cartilage in tension. *J Biomech Eng* 2002;124:223–8.
- [32] Urayama K, Takigawa T, Masuda T. Poisson's ratio of poly(vinyl alcohol) gels. *Macromolecules* 1993;26:3092–6.
- [33] Hayes WC, Keer LM, Herrmann G, Mockros LF. A mathematical analysis for indentation tests of articular cartilage. *J Biomech* 1972;5:541–51.
- [34] Spiller KL, Laurencin SJ, Charlton D, Maher SA, Lowman AM. Superporous hydrogels for cartilage repair. Evaluation of the morphological and mechanical properties. *Acta Biomaterialia* 2008;4:17–25.